

Quantification of retinal artery-vein ratio for vascular disease diagnosis using spatial U-Net

Lakshmi Kala Pampana, Manjula Sri Rayudu

Department of Electronics, Communication Engineering, Electronics and Instrumentation Engineering,
Vallurupalli Nageswara Rao Vignana Jyothi Institute of Engineering and Technology, Telangana, India

Article Info

Article history:

Received Mar 26, 2022

Revised Jun 24, 2022

Accepted Jul 8, 2022

Keywords:

Biomarkers

Classification

Life threat risk factors

Spatial segmentation

Systemic disorders

Vascular caliber

ABSTRACT

The retinal vascular morphological caliber changes reveal the signs of systemic health disorder and life threat diseases such as cardio and cerebral diseases. The quantitative vascular parameters like narrowed arteries, widened venules, reduced artery-vein ratio (AVR) have been associated with aforesaid disorders and diseases. Hence the quantitative biomarker AVR is important parameter in diagnosing variety of diseases. The accurate quantification of AVR be possible if and only if accurate classification of arteries and vein is done. In this paper, we proposed a deep learning based robust vessel segmentation and classification algorithm based on spatial U-Net and the accuracy of the algorithm is 97.8%. In the quantification process, this algorithm is applied on region of interest (RoI) of a fundus image and measured the AVR values using central retinal artery equivalent (CRAE) and central retinal vein equivalent (CRVE). The experimentation is carried on the digital retinal images for vessel extraction (DRIVE) dataset. The outcome of this work is the AVR observed to be >0.4 in normal retinal case and AVR value <0.4 for unhealthy case.

This is an open access article under the [CC BY-SA](https://creativecommons.org/licenses/by-sa/4.0/) license.



Corresponding Author:

Lakshmi Kala Pampana

Department of Electronics, Communication Engineering and Electronics, and Instrumentation

Engineering, VNR Vignana Jyothi Institute of Engineering and Technology

Hyderabad, Telangana-500090, India

Email: kala.pampana@gmail.com

1. INTRODUCTION

The retinal microvasculature provides an easily accessible location for non-invasive microcirculation assessment. Some investigations have found a link between some of the retinal vessel calibre alterations like retinal artery narrowing, venule widening, reduced artery vein ratio (AVR) and hypertensive retinopathy, coronary heart disease (CHD) [1]-[3]. According to Blue Mountain Eye Studies (BMES) [4], a high value of AVR indicates that arteriolar and venular calibres in that eye are on average the same, whereas a lower AVR indicates that arterioles are smaller than venules or venules are wider than arterioles. Due to arterial hypertension the arteries are getting narrowed over the period. Narrowed arteries itself is a biomarker for coronary artery disease in women [5]. Hence these kind of structural alterations in retinal vessel calibre provide quantitative biomarkers for diagnosing different systemic health disorders as well as a few cardiovascular diseases. The quantitative measurement of AVR biomarker requires the measurement of artery and vein diameters within the region of interest (RoI) on the retinal image. Within the RoI the arteries and veins are segmented and classified. Some of the existing methodologies for segmenting the vessels based on the traditional image processing methods are matched filtering, a multi-scale method and morphological processing. Chaudhuri *et al.* [6] suggested a strategy that involved searching for vessel segments in all available directions using different templates. Rangayyan [7] classified the pixels using

multilayer perceptron using the features extracted from Gabor filtering on green channel of the fundus images. Niemeijer *et al.* [8] developed a method for grading blood vessels that combined the k-nearest neighbour classifier using first and second order derivatives of a matched Gaussian filter. Hatanaka *et al.* [9] proposed a double ring filter and black hat transform based method. Hatanaka *et al.* [10] developed a system in which the artery and vein classification is done based on linear discriminant analysis (LDA). Vázquez *et al.* [11] classified the vessels using minimal path and measured at different distances from optic disc. All these methods for vessel segmentation depends upon ability of feature extraction methods and the type of filters for segmenting and classifying the vessels.

The accurate quantification of arteriovenous (AV) ratio is essential in diagnosing the levels of abnormality from the retinal images. It depends upon the method where precise classification can be done on each pixel as artery and vein. Most recently deep learning algorithms performs the task of classifying the vessels as arteries and veins precisely. The most relevant tasks like feature extraction pertaining to segmentation is done by the neural network itself. Both local and global features are extracted using this approach. The U-Net [12] and its variants [13]-[15] outperforms the segmentation and classification tasks on each pixel. Hu *et al.* [16] proposed a segmentation and classification task based on vessel constraint network in which a feature weight map and multiscale modules are used along with U-Net variant. Here the pixels are segmented by combining both local and global features at different resolution levels. Hence some of the noisy edges also classified properly as arteries and veins. We proposed a spatial U-Net based classifier for segmenting blood vessels as arteries and veins. This method better classifies the pixel as arteries and veins even in the noisy and ambiguous areas.

The existing methods in the quantification of AVR are discussed below. Manikis *et al.* [17] proposed a blood vessel detection method through top hat transform and median filter on VICAVR database. Agurto *et al.* [18] used a hessian-based vessel segmentation technique with thresholding to achieve their results. It was put to the test on two different datasets: digital retinal images for vessel extraction (DRIVE) and structured analysis of the retina (STARE). Based on a multi-scale enhancement and local-entropy thresholding, Khitran *et al.* [19] developed an automated vessel segmentation approach. The AVR calculation is carried on six largest vessels within the RoI of 0.5 DD to 1 DD. Rani and Mittal [20] classified blood vessels as arteries and veins with a new feature vector. Their experimentation is carried on both VICAVR and DRIVE datasets. Ramanathan *et al.* [21] have segmented and classified the vessels based on top hat transform and iterative thresholding's on Messidor database. The methods discussed for segmentation and classification so far are based on different manual processing techniques and listed in Table 1. The segmentation and classification accuracies depend upon the manual setting of filter parameters. Hence the accuracy of AVR ratio is also limited by that of segmentation and classification techniques. Recently deep learning-based algorithms outperforms in the field of different medical imaging application [22]-[24]. In this paper, we proposed a deep learning based spatial U-Net for segmentation and classification. Here, the optimized filter parameters are obtained by iterative training of the neural network. Hence, the blood vessels are classified accurately so as the quantification of central retinal artery equivalent (CRAE), central retinal vein equivalent (CRVE) and AVR.

Table 1. Comparison of existing methods in the quantification of AVR

Author	Method	Dataset	AVR	
			Normal	Abnormal
Narasimhan <i>et al.</i> ,[31]	Median filter, Top hat transform	VICAVR	0.6-0.7	0.24-0.49
Manikis <i>et al.</i> ,[17]	CLAHE, Hessian based vessel segmentation	DRIVE/STARE	-	0.1-0.5
Agurto <i>et al.</i> ,[26]	Multi-scale linear structure, Enhancement	Clinically acquired	0.67	0.58
Khitran <i>et al.</i> ,[27]	Gabor wavelet, multi layered thresholding	VICAVR DRIVE	-	0.1-0.5
Rani <i>et al.</i> ,[28]	Top hat transform and iterative thresholding	MESSIDOR	0.62-0.735	0.203-0.495

2. METHOD

AVR quantification requires accurate classification of pixels as arteries and veins hence as a starting step, a robust segmentation and classification method is developed using spatial U-Net architecture with structured dropouts and activation block concept. After localizing the optic disc using circular hough transform (CHT), the RoI is determined as 1 disc diameter (DD) to 1.5 DD from the optic disc as per Knudtson's formulae [25]. Within this RoI, the arteries and veins are differentiated by applying the developed classification methods. Usually, six largest arteries and veins are considered for quantification and CRAE and CRVE are calculated. Finally, AVR is measured from the ratio of CRAE and CRVE. The proposed model for quantification of AVR is depicted in Figure 1.

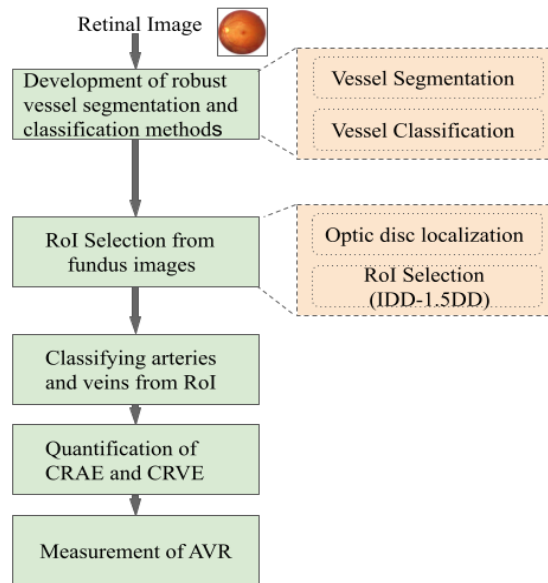


Figure 1. Proposed method for quantification of AVR

2.1. Vessel segmentation and classification

In the proposed method, vessels are extracted and classified using the spatial U-Net architecture which is empowered by structured dropout and activation block as shown in Figure 2. Basically, U-Net is configured with down sampling and up sampling convolutional blocks. At each step of down sampling path, the convolution operation, regularization using structured dropouts, batch normalization and a 2×2 max pooling are carried.

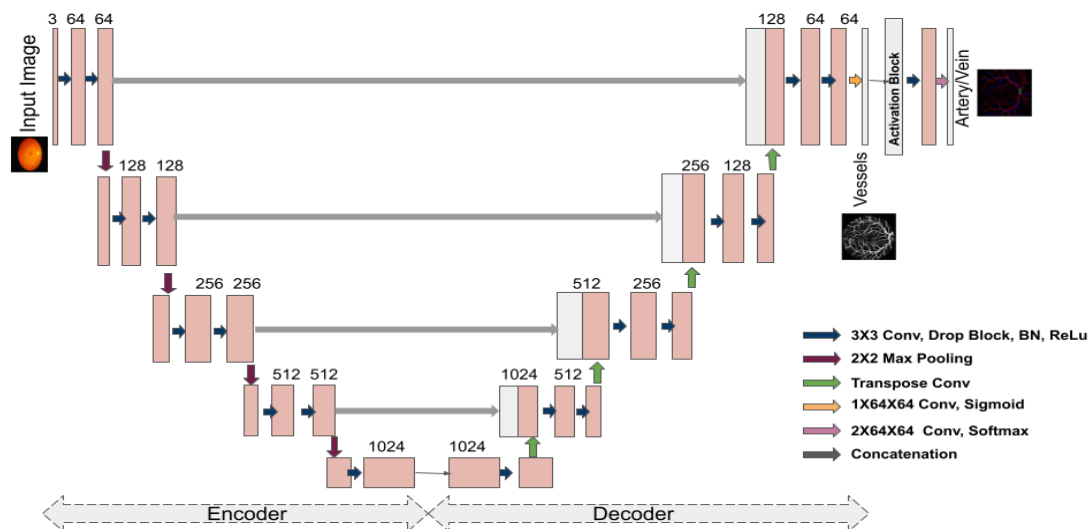


Figure 2. Proposed method to classify arteries and veins

In this process as move on to the deeper layers the feature maps are doubled with low resolution. Even though at the deeper layers the feature maps are of low resolution, but they contain semantically quality feature information. Later at each step of the up-sampling path, the semantically rich features are concatenated with the same level of resolution from the down sampling path. In this path a 2×2 transposed convolution operation is carried at each step of up sampling path. This concatenation operation makes the U Net can perform more robust vessel segmentation. Then the spatial activation block classifies the arteries and veins from the vessel background.

2.1.1. Structured dropouts

Random and Structured dropouts as shown in Figure 3. The model’s overfitting can be reduced by the technique called regularization. In this process, some of the neurons are randomly dropped while training progress from one epoch to another epoch. The weights of those neurons made equal to 0. The original image and random dropouts from the convolution layer are shown in Figure 3(a) and Figure 3(b). But in our work, we used structured dropout instead of random dropout. In the structured dropout a feature map layer is dropped instead of single neuron as shown in Figure 3(c). The probability $p=0.2$ set at the input layer, $p=0.5$ for the hidden layers. The structured dropouts are configured as per the equation given in 1 and 2.

- During training phase:

$$Z = f(Wy) \circ m, m_i \sim Bernoulli(p) \tag{1}$$

- During testing phase:

$$Z = (1 - p)f(Wy) \tag{2}$$

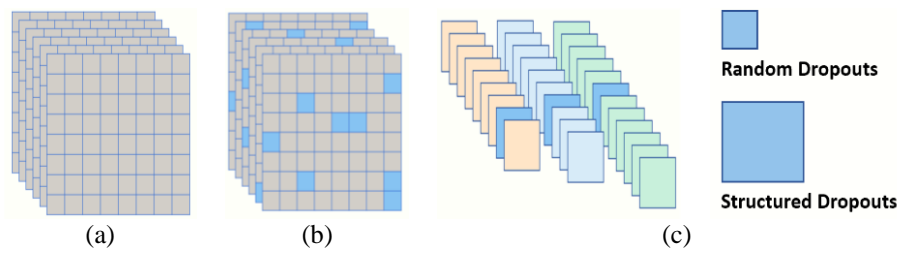


Figure 3. Random and Structured dropouts (a) original image, (b) random dropouts, and (c) structured dropouts

2.1.2. Objective function

The objective function is iterated for different epochs by choosing best set of hyper parameters are thereby decreasing the objective function to its lowest value. During training, the classifier computes the cross-entropy loss for each of the N points in the training set, effectively fitting the distribution \hat{t}_i . Because each point's probability is $1/N$, cross-entropy is expressed as (3).

$$L_{BCE}(\hat{t}_i, i) = -\frac{1}{N} \sum (i_i \log(\hat{t}_i) + (1 - i_i) \log(1 - \hat{t}_i)) \tag{3}$$

The dice loss is preferable for segmenting task when imbalanced pixels in the image. As the artery vein area is 10-15% of overall background on the retinal image, we considered dice loss function while training and is computed as given (4) and (5). The combined loss function is given in (6).

$$L_{Dice}(\hat{t}_i, i) = 1 - DiceCoef \tag{4}$$

$$DiceCoef = \frac{2 \sum_i i_i \hat{t}_i}{\sum_i (i_i + \hat{t}_i)} \tag{5}$$

$$Total Loss (L_{total loss}) = LB_{CE}(\hat{t}_i, i) + L_{Dice}(\hat{t}_i, i) \tag{6}$$

Where i_i ground truth and \hat{t}_i is the predicted values.

2.2. Region of interest (RoI) determination

In the process of RoI determination, first optic disc location needs to be identified. Through which all the blood vessels enters/leaves into/from brain. The vessels from optic disc spans over the retina till the periphery region. As per the literature, the vessel within 1-disc diameters (1-DD) serves as biomarkers for diagnosing many diseases. So, we have chosen Roni as 0.5-disc diameter to one-disc diameters from the optic disc. Then the arteries and veins are segmented and classified. The optic disc localization and RoI are shown in Figure 4.

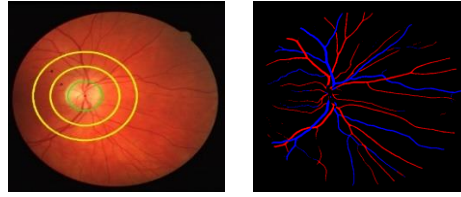


Figure 4. RoI determination and classification

2.3. Measurement of vessel calibre

The vessel calibre measurements are carried using Knudtson's formulae. The artery and vein calibre parameters CRAE and CRVE is measured within the RoI. The approximate artery and vein calibre according to Knudtson's as given in (7) and (8).

$$CRAE = 0.88 * (w_{a1}^2 + w_{a2}^2)^{1/2} \quad (7)$$

$$CRVE = 0.95 * (w_{v1}^2 + w_{v2}^2)^{1/2} \quad (8)$$

Where w_{a1} , w_{a2} and w_{v1} , w_{v2} are the widths of largest and smallest arteries and veins. Then for the measurement of CRAE, CRVE the following procedure is adopted. First six largest arteries are considered from the RoI. Out of which one smallest artery and one largest artery is considered and measured the Euclidean distance to find the individual artery width following measuring of equivalent width using (1). From the remaining 5 arteries again the next set of largest and smallest arteries are considered, measured the equivalent width, and then continue till the final width measurement, that is the measurement of CRAE. A similar process is carried for the measurement of CRVE using the (2).

2.4. Quantification of AVR

The precise and accurate classification of a retinal image as healthy or unhealthy is depends on the accurate quantification of AVR. It inturn depends on the retinal vessel central equivalents CRAE and CRVE computation equation. The diagnosing parameters from the retinal images are CRAE, CRVE and AVR for the biomarkers of artery narrowing, venule widening and reduced AVR. Respectively. The artery-vein ratio (AVR) is defined as the ratio of central retinal artery equivalent (CRAE) and central retinal vein equivalent (CRVE) and is given in (9).

$$AVR = \frac{CRAE}{CRVE} \quad (9)$$

As the RoI is considered between 0.5 DD to 1 DD, the measurements are focused on central retinal equivalent measures. For other systemic abnormalities the periphery region of the eye also affected then the RoI selection depends upon the field of view (FoV). With the recent ultra-wide retinal imaging methods, the FoV can also be increased. Finally, the quantified score of AVR is used to deduce the qualitative inference. i.e lower AVR value, less than 0.5 may be the indication of hypertension according to Keith Wagener Barker. Even narrowed arteries and widened venules either individually or combinedly are the biomarkers for systemic hypertension and stroke events. Hence this quantitative measurement provides a biomarker for diagnosing different non-ocular diseases.

3. RESULTS AND DISCUSSION

3.1. Dataset

Our experimentation is carried on DRIVE [26] dataset for AVR measurement. The dataset has 40 colour fundus images of resolution 584×565. Out of 40 images, 20 images are used for training and remaining 20 for testing. While training the neural network, the small image patches are extracted from the retinal images and those are given to neural network. The network extracts all the global and minute features required for classification. The network training progress is monitored for best optimized objective function and chosen the best epoch as 400 with learning parameter 0.001, convergence rate 0.9 with the stochastic gradient optimized algorithm. The original images and their classification results are shown in Figure 5.

The model's has given the performance metrics like sensitivity, specificity, and accuracy for segmenting the vessels from background are 0.8310, 0.9867, 0.9557 respectively and that of classification

results are 0.9423, 0.9556, 0.9788. The models performance in segmenting and classifying the arteries and veins are compared with the existing methods [27]-[30] and are shown in Figure 6. Our artery-vein classification network based on Spatial U Net has shown 97.8 % accurate classification result. Hence this method supports for the quantification process of AVR accurately.

The vessel width is measured from the region of interest 1-DD to 1.5DD from the optic disc. The usual optic disc width is 1850 μm . From the optic disc within the zone B, the arteries and vein central equivalents (CRAE, CRVE) are measured and computed the AVR as shown in (1)-(3). On DRIVE dataset for each image, AVR value is computed statistically and listed in Table 1. According to Keith and Wegner [31] images having the AVR value >0.667 are healthy individuals and other images are having <0.667 are from unhealthy individuals indicating that their vessel calibre is deviating from normal calibre, at the same time may be the indication of systemic health disorder initially. Through our experimentation we observed 4 images have AVR value <0.4 and upon observation these images are observed visually some pathological changes and is shown in Figure 7.

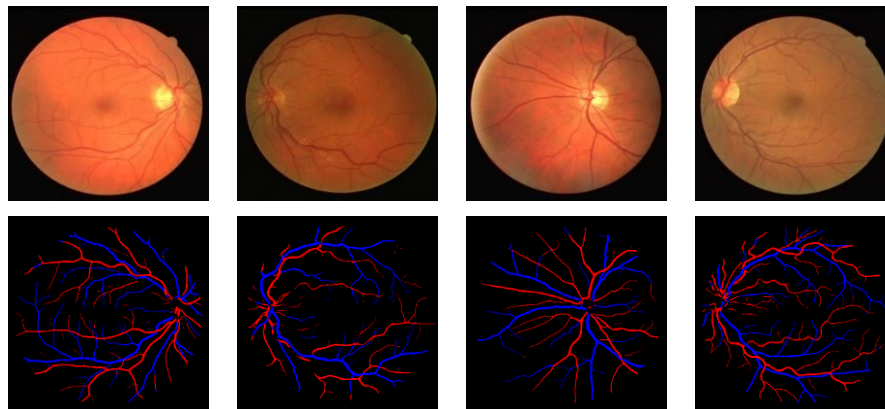


Figure 5. Original and classified images on DRIVE dataset

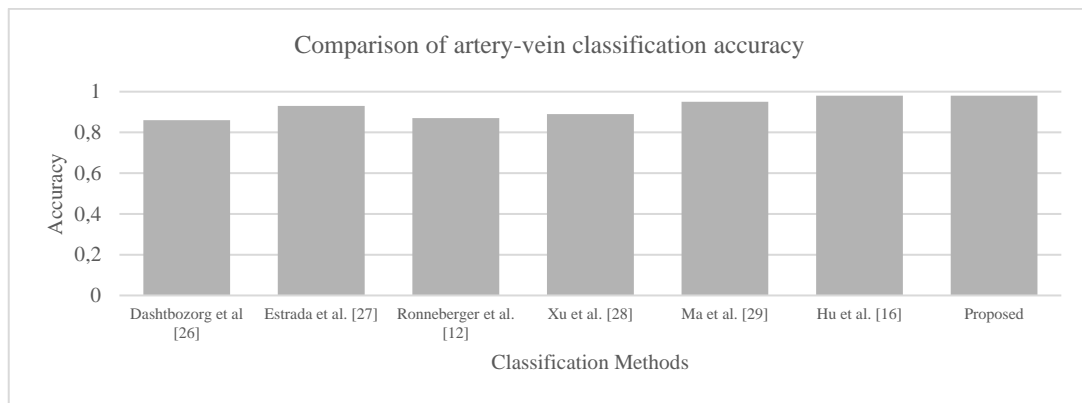


Figure 6. Comparison of artery-vein classifier's performance with existing methods



Figure 7. AVR measurements on pathological images from DRIVE dataset

4. CONCLUSION

The vascular morphological calibre changes reveal the signs of systemic health disorder and life threat diseases these diseases. In this work, the prominent and quantitative biomarkers such as CRAE, CRVE and AVR are measured on different images to know the early signs of disorders and diseases. The accurate quantification of AVR depends on the accuracy of the model in classifying the vessels as arteries and veins. Hence, we proposed a robust artery vein classification model based on Spatial attention U Net architecture. The vessel widths are measured in terms of number of pixels after successfully employing the proposed method of classification. It has been observed that 4 pathological images are having AVR less than 0.4, indicating that there are considerable vessel calibre changes along with other diabetic retinopathy changes.

ACKNOWLEDGEMENTS

We would like to convey our deep gratitude towards our college management for providing us resources to carry the research work.





REFERENCES

- [1] E. T. Reiner, M. Strozzi, B. Skoric, and Z. Reiner, "Relation of Atherosclerotic changes in retinal arteries to the extent of coronary artery disease," *The American Journal of Cardiology*, vol. 96, no. 8, pp. 1107–1109, Oct. 2005, doi: 10.1016/j.amjcard.2005.05.070.
- [2] B. B. Duncan, T. Y. Wong, H. A. Tyroler, C. E. Davis, and F. D. Fuchs, "Hypertensive retinopathy and incident coronary heart disease in high risk men," *British Journal of Ophthalmology*, vol. 86, no. 9, pp. 1002–1006, Sep. 2002, doi: 10.1136/bjo.86.9.1002.
- [3] J. J. Wang *et al.*, "Retinal vascular calibre and the risk of coronary heart disease-related death," *Heart*, vol. 92, no. 11, pp. 1583–1587, Nov. 2006, doi: 10.1136/hrt.2006.090522.
- [4] N. Joachim, P. Mitchell, G. Burlutsky, A. Kifley, and J. J. Wang, "The Incidence and progression of age-related macular degeneration over 15 Years," *Ophthalmology*, vol. 122, no. 12, pp. 2482–2489, Dec. 2015, doi: 10.1016/j.ophtha.2015.08.002.
- [5] T. Y. Wong *et al.*, "Retinal arteriolar narrowing and risk of coronary heart disease in men and women: *The Atherosclerosis Risk in Communities Study*," *Journal of the American Medical Association*, vol. 287, no. 9, pp. 1153–1159, Mar. 2002, doi: 10.1001/jama.287.9.1153.
- [6] S. Chaudhuri, S. Chatterjee, N. Katz, M. Nelson, and M. Goldbaum, "Detection of blood vessels in retinal images using two-dimensional matched filters," *IEEE Transactions on Medical Imaging*, vol. 8, no. 3, pp. 263–269, 1989, doi: 10.1109/42.34715.
- [7] R. M. Rangayyan, "Detection of blood vessels in the retina with multiscale Gabor filters," *Journal of Electronic Imaging*, vol. 17, no. 2, p. 023018, 2008, doi: 10.1117/1.2907209.
- [8] M. Niemeijer, J. Staal, B. V. Ginneken, M. Loog, and M. D. Abramoff, "Comparative study of retinal vessel segmentation methods on a new publicly available database," in *Medical Imaging 2004: Image Processing*, May 2004, vol. 5370, p. 648, doi: 10.1117/12.535349.
- [9] Y. Hatanaka, H. Tachiki, K. Ogohara, C. Muramatsu, S. Okumura, and H. Fujita, "Artery and vein diameter ratio measurement based on improvement of arteries and veins segmentation on retinal images," *Proceedings of the Annual International Conference of the IEEE Engineering in Medicine and Biology Society, EMBS*, vol. 2016-October, pp. 1336–1339, 2016, doi: 10.1109/EMBC.2016.7590954.
- [10] Y. Hatanaka *et al.*, "Automated blood vessel extraction using local features on retinal images," *Medical Imaging 2016: Computer-Aided Diagnosis*, vol. 9785, p. 97852F, 2016, doi: 10.1117/12.2216572.
- [11] S. G. Vázquez *et al.*, "Improving retinal artery and vein classification by means of a minimal path approach," *Machine Vision and Applications*, vol. 24, no. 5, pp. 919–930, Jul. 2013, doi: 10.1007/s00138-012-0442-4.
- [12] O. Ronneberger, P. Fischer, and T. Brox, "U-net: Convolutional networks for biomedical image segmentation," in *Lecture Notes in Computer Science (including subseries Lecture Notes in Artificial Intelligence and Lecture Notes in Bioinformatics)*, vol. 9351, 2015, pp. 234–241.
- [13] B. Wang, S. Qiu, and H. He, "Dual encoding U-Net for retinal vessel segmentation," in *Lecture Notes in Computer Science (including subseries Lecture Notes in Artificial Intelligence and Lecture Notes in Bioinformatics)*, vol. 11764 LNCS, 2019, pp. 84–92.
- [14] J. Zhuang, "LadderNet: Multi-path networks based on U-Net for medical image segmentation," *arXiv preprints*, Oct. 2018, [Online]. Available: <http://arxiv.org/abs/1810.07810>.
- [15] C. Guo, M. Szemenyei, Y. Yi, W. Wang, B. Chen, and C. Fan, "SA-UNET: Spatial attention U-net for retinal vessel segmentation," in *Proceedings-International Conference on Pattern Recognition*, Jan. 2020, pp. 1236–1242, doi: 10.1109/ICPR48806.2021.9413346.
- [16] J. Hu *et al.*, "Automatic artery/vein classification using a vessel-constraint network for multicenter fundus images," *Frontiers in Cell and Developmental Biology*, vol. 9, Jun. 2021, doi: 10.3389/fcell.2021.659941.
- [17] G. C. Manikis *et al.*, "An image analysis framework for the early assessment of hypertensive retinopathy signs," *2011 E-Health and Bioengineering Conference, EHB 2011*, pp. 1–6, 2011.
- [18] C. Agurto, V. Joshi, S. Nemeth, P. Soliz, and S. Barriga, "Detection of hypertensive retinopathy using vessel measurements and textural features," in *2014 36th Annual International Conference of the IEEE Engineering in Medicine and Biology Society, EMBC 2014*, Aug. 2014, pp. 5406–5409, doi: 10.1109/EMBC.2014.6944848.
- [19] S. Khitran, M. U. Akram, A. Usman, and U. Yasin, "Automated system for the detection of hypertensive retinopathy," in *2014 4th International Conference on Image Processing Theory, Tools and Applications, IPTA 2014*, Oct. 2015, pp. 1–6, doi: 10.1109/IPTA.2014.7001984.
- [20] A. Rani and D. Mittal, "Measurement of Arterio-venous ratio for detection of hypertensive retinopathy through digital color fundus images," *Journal of Biomedical Engineering and Medical Imaging*, vol. 2, no. 5, Oct. 2015, doi: 10.14738/jbemi.25.1577.





- [21] T. T. Ramanathan, M. J. Hossen, M. S. Sayeed, and J. E. Raja, "A deep learning approach based on stochastic gradient descent and least absolute shrinkage and selection operator for identifying diabetic retinopathy," *Indonesian Journal of Electrical Engineering and Computer Science*, vol. 25, no. 1, pp. 589–600, Jan. 2022, doi: 10.11591/ijeecs.v25.i1.pp589-600.
- [22] U. W. Wasekar and R. K. Bathla, "A review on supervised learning methodologies for detection of exudates in diabetic retinopathy," *Indonesian Journal of Electrical Engineering and Computer Science*, vol. 23, no. 2, p. 837, Aug. 2021, doi: 10.11591/ijeecs.v23.i2.pp837-846.
- [23] M. Mohebbanaaz, Y. P. Sai, and L. V. R. Kumari, "Detection of cardiac arrhythmia using deep CNN and optimized SVM," *Indonesian Journal of Electrical Engineering and Computer Science*, vol. 24, no. 1, p. 217, Oct. 2021, doi: 10.11591/ijeecs.v24.i1.pp217-225.
- [24] K. MD, L. Ke, H. LD, W. TY, K. R. and K. Be, "Revised formulas for summarizing retinal vessel diameters.," *Current eye research*, vol. 27, no. 3, pp. 143–149, 2003.
- [25] S. Joes, *et al.* "Ridge-based vessel Segmentation in Color Images of the Retina," *IEEE Transactions on Medical Imaging*, vol. 23, no. 4, pp. 501–509, Apr. 2004, doi: 10.1109/TMI.2004.825627.
- [26] B. Dashtbozorg, A. M. Mendonca, and A. Campilho, "An Automatic graph-based approach for artery/vein classification in retinal images," *IEEE Transactions on Image Processing*, vol. 23, no. 3, pp. 1073–1083, Mar. 2014, doi: 10.1109/TIP.2013.2263809.
- [27] R. Estrada, M. J. Allingham, P. S. Mettu, S. W. Cousins, C. Tomasi, and S. Farsiu, "Retinal artery-vein classification via topology estimation," *IEEE Transactions on Medical Imaging*, vol. 34, no. 12, pp. 2518–2534, Dec. 2015, doi: 10.1109/TMI.2015.2443117.
- [28] X. Xu *et al.*, "Simultaneous arteriole and venule segmentation with domain-specific loss function on a new public database," *Biomedical Optics Express*, vol. 9, no. 7, p. 3153, Jul. 2018, doi: 10.1364/BOE.9.003153.
- [29] W. Ma, S. Yu, K. Ma, J. Wang, X. Ding, and Y. Zheng, "Multi-task neural networks with spatial activation for retinal vessel segmentation and artery/vein classification," in *Lecture Notes in Computer Science (including subseries Lecture Notes in Artificial Intelligence and Lecture Notes in Bioinformatics)*, vol. 11764 LNCS, 2019, pp. 769–778.
- [30] N. M. Keith, H. P. Wagener, and N. W. Barker, "Some different types of essential hypertension: their course and prognosis," *American Journal of the Medical Sciences*, vol. 268, no. 6, pp. 336–345, Dec. 1974, doi: 10.1097/00000441-197412000-00004.
- [31] K. Narasimhan, V. C. Neha, and K. Vijayarekha, "Hypertensive retinopathy diagnosis from fundus images by estimation of avr.," *Procedia Engineering*, vol. 38, pp. 980–993, 2012, doi: 10.1016/j.proeng.2012.06.124.

BIOGRAPHIES OF AUTHORS



Lakshmi Kala Pampana     is a full-time research scholar in dept. of ECE working at Research Center VNR Vignana Jyothi Institute of Engineering and Technology under JNTU, Hyderabad, India. She received her M. Tech in VLSI System Design from JNTU and B. Tech in ECE from JNTU, Hyderabad, India. Her research interests include image processing, artificial intelligence, machine learning and deep learning. Se can be contacted at email: kala.pampana@gmail.com.



Dr. Manjula Sri Rayudu     is a Professor and Head in the Department of Electronics and Instrumentation Engineering, VNR VJIET, Hyderabad. She Received PhD from JNTUH, M.E from AU and BTech from JNTUK. She has 23 years of teaching experience including 10 years of Research. She has over thirty research papers in numerous journals and conference proceedings to her credit. She has three funding projects under AICTE & UGC and two Patents were published under her Credit. She is a Senior IEEE Member, Member IEEE WIE AG, IEEE EMBS Member, Fellow of IETE, life member of ISTE, life member of instrumentation society of India (ISOI). She can be contacted at email: manjulasree_r@vnrvjiet.in.